

# Dropout Prediction Variation Estimation Using Neuron Activation Strength

Haichao Yu\*  
UIUC  
haichao3@illinois.edu

Zhe Chen\*  
Google, Inc.  
chenzhe@google.com

Dong Lin\*  
Google, Inc.  
dongl@google.com

Gil I. Shamir  
Google, Inc.  
gshamir@google.com

Jie Han  
Google, Inc.  
jih@google.com

## ABSTRACT

It is well-known that deep neural networks generate different predictions even given the same model configuration and training dataset. It thus becomes more and more important to study prediction variation, the variation of the predictions on a given input example, in neural network models. Dropout has been commonly used in various applications to quantify prediction variations. However, using dropout in practice can be expensive as it requires running dropout inferences many times to estimate prediction variation.

We study how to estimate dropout prediction variation in a resource-efficient manner. We demonstrate that we can use neuron activation strengths to estimate dropout prediction variation under different dropout settings and on a variety of tasks using three large datasets, MovieLens, Criteo, and EMNIST. Our approach provides an inference-once alternative to estimate dropout prediction variation as an auxiliary task. Moreover, we demonstrate that using activation features from a subset of the neural network layers can be sufficient to achieve variation estimation performance almost comparable to that of using activation features from all layers, thus reducing resources even further for variation estimation.

## KEYWORDS

Dropout, Neural Networks, Neuron Activation, Prediction Uncertainty, Prediction Variation

## 1 INTRODUCTION

Deep neural networks (DNNs) have achieved impressive performance and gained wide adoption in a variety of tasks in recent years. However, it is known that given the same model configuration and training dataset, DNNs can produce different predictions for the same input example if there are training differences [3, 6, 9, 30, 39, 43–45, 47, 52]. Such differences can emerge from different initialization, data orderings and shuffling, distributed and parallelized training, parameter update schedules, round off errors and more. Techniques that do change the training configuration and data like data augmentation and regularization can further enhance such differences. It thus becomes more and more important to study prediction variation in neural network models [26, 42]. We define **prediction variation (PV)** as a measure that describes the variations of the model predictions on the given input example.

Ensemble and dropout are two popular methods for prediction variation estimation [2, 14, 30], but both are expensive to deploy in

practice. The ensemble approach [2, 30] trains and deploys multiple model copies which are often different on parameter initialization or training data order. These multiple model copies or ensemble members produce a set of predictions for a given example and these predictions can be used to generate prediction variation measurements. Unlike ensembles, the dropout approach [14, 31] trains one copy of the model using a given dropout rate  $r$ . During inference time, the dropout approach runs multiple inferences with the dropout rate  $r$  to obtain a collection of predictions from which prediction variation is measured. This step to obtain **dropout prediction variation (DPV)** is expensive as it requires running multiple inferences for a given example to calculate the DPV.

Many researchers have studied reducing the cost to estimate ensemble based prediction variation [1, 6, 34, 49, 52]. For example, [6] demonstrated that it is possible to use **neuron activation strength** features to infer ensemble prediction variation. Such inference serves as an auxiliary task to the main learning task. Instead of training multiple copies of the model, and using each copy for inference, the auxiliary task was trained to estimate the ensemble prediction variation using the *post neurons activation* values of the target prediction task network. To the best of our knowledge, reducing cost of DPV measures has been an open problem.

**Our Goal** — We study reducing the inference cost of estimating dropout prediction variation by using neuron activation strengths. We focus on prediction variations generated by dropout for the reasons described below:

Dropout is cheaper to train than ensembles, requiring fewer training, memory and storage resources. Ensemble methods, as shown in [6], can be reduced in deployment to a learned auxiliary task that predicts the ensemble PV score. However, such methods still require training an ensemble of multiple model copies on the target task to obtain the PV labels, in order to train the auxiliary task. On the other hand, it is cheaper to obtain the PV labels using the dropout approach to train the auxiliary task.

While ensembles have been used for PV estimation, dropout prediction variation is gaining popularity for a wide variety of real-world applications. [51] used DPV to detect untrustable configurations for molecular simulations to aid quantitative design of materials and devices. In [16], DPV was used for active learning applications, as active learning methods generally rely on uncertainty scores which guides learning and updates of models from small amounts of training data. [32] used DPV to improve computer-aided diagnoses and their robustness for patient safety.

\* Authors contributed equally.

Finally, ensembles can be constructed in multiple ways, where each can have its unique PV score. Dropout is generally viewed as one type of ensemble (more discussion in Section 6). While PV scores may differ between ensembles and dropout, our focus in this paper is not on such differences, but on providing a cost-efficient way to measure DPV.

**Challenges** — We address the following challenges or questions:

*Various tasks* — Dropout prediction variation has a wide range of real-life application scenarios. Thus, we study DPV estimation for a variety of tasks, and demonstrate our approach on three large datasets, MovieLens, Criteo, and EMNIST.

*DPV estimation* — We study DPV for various configurations and hyperparameters. For example, one can train the target task with or without dropout, and different dropout rates can be used.

*Activation strength features* — We begin by showing how activation strengths of all neurons from fully-connected layers in the network can be used to estimate PV. However, using all the activation features may be impractical for very large neural networks [21, 24]. We thus continue by showing that DPV can be estimated even with a small subset of all the activation features.

**Our Approach** — We consider a learning framework which performs two tasks: a) the target task that optimizes the primary prediction objectives using DNNs, and b) the variation estimation task that serves as an auxiliary task to estimate DPV. The neural network based variation estimation task takes neuron activation strengths from the target task as the input features, and is trained with DPV labels. We collect the DPV labels on a dropout-enabled target task by running multiple inferences with a predetermined dropout rate for each example. For each inference, a different drawing of the random dropout can give a slightly different prediction from other inferences.

Training of the variation estimation task model requires running multiple inferences on a dropout-enabled target task model to generate the DPV labels. However, the deployed variation estimation task performs a single inference for an example to estimate its DPV score, thus serving as a cost-efficient auxiliary task. We further simplify the auxiliary task by reducing its input to only include a subset of the neuron layers in the network of the target task.

We test our approach on regression, binary classification, and multi-class classification target tasks. These tasks are based on the recommender system benchmark dataset MovieLens; the Ads click-through rate binary prediction dataset Criteo dataset; and the benchmark image digit recognition dataset EMNIST. We show that our estimation method can be used with different dropout settings on these benchmark datasets. We observe strong  $R^2$  correlations between our method and the true dropout labels in almost all settings. In particular, our approach achieves strong accuracy (0.8 to 0.9) in identifying whether an example has very high or very low dropout prediction variations. Furthermore, substantial reduction of the input size by using only a subset of the neurons also leads to similar results.

**Contributions** — Our contributions are:

- We propose two configuration setups for the dropout prediction variation estimation task by considering whether the target task is trained with dropout (Section 3).

- We demonstrate that the proposed resource-efficient method provides good estimates of the true dropout variation scores on three large public datasets (Section 5).
- We show that even a reduced complexity form of our method, using a fraction of neuron activations, still achieves reliable estimates of the true DPV scores (Section 5).

We discuss related work in Section 2, introduce the dropout variation estimation framework in Section 3, present the experiment setup in Section 4, the experiment results in Section 5, discuss dropout vs ensemble in Section 6, and conclude in Section 7.

## 2 RELATED WORK

**Uncertainty estimation** [17] is emerging as a very important topic in machine learning with a wide range of applications [4, 11, 27, 32, 51, 54]. For example, in [54], uncertainty sampling was employed to increase the diversity of selected training data. [27] incorporated uncertainty into the cost function for reinforcement learning of autonomous robots to reduce the number of dangerous collisions. [10] examined uncertainty estimation for brain tumor segmentation to calibrate volume estimates.

Uncertainty in machine learning models can lead to **prediction variations** or model prediction disagreements [10, 12, 14]. Recent work [3, 9, 43–45, 47] has focused on levels of **irreproducibility** in deep models, where it was observed that nondeterminism in training of deep models leads to even larger levels of prediction differences. Designing systems that are able to measure the cumulative prediction variations is, therefore, very important, as such systems can be designed to compensate for such variations.

A large volume of uncertainty estimation studies has been under the **Bayesian umbrella** [5, 23, 29, 40], where inference also provides an uncertainty score. Direct Bayesian inference is usually impossible as posterior distributions over model parameters are generally intractable. Some classical Bayesian approaches, such as Markov Chain Monte Carlo, rely on sampling but generally do not scale well with large DNNs [41]. Instead, approximations, such as variational inference [5, 23, 29, 40], can be used. It is not clear, however, how accurately such approximations capture PV.

**Ensembles** emerged as another class of methods for uncertainty estimation [30, 49, 52]. They are, in fact, a form of Bayesian mixture [53]. An ensemble estimates uncertainty through the distribution of predictions of multiply trained copies of the same model. While ensembles can provide effective PV scores, they increase both the training and deployment complexities, and may be impractical in some real large-scale systems. Researchers have proposed various methods to reduce computational cost [6, 20, 35, 49, 52]. For example, [49] proposed to ensemble only the last several layers to approximate a deep model ensemble, and [52] proposed BatchEnsemble to reduce ensemble complexity by sharing weights among ensemble members. Such simplifications are usually associated with some cost due to the complexity reduction. In practical large scale systems, reducing the total number of weights, as proposed by these methods, normally degrades inference accuracy. In [6], it was proposed to reduce the costs of ensemble deployment by training an auxiliary model on the PV scores of multiple trained copies of the model. This reduced inference costs, but still required

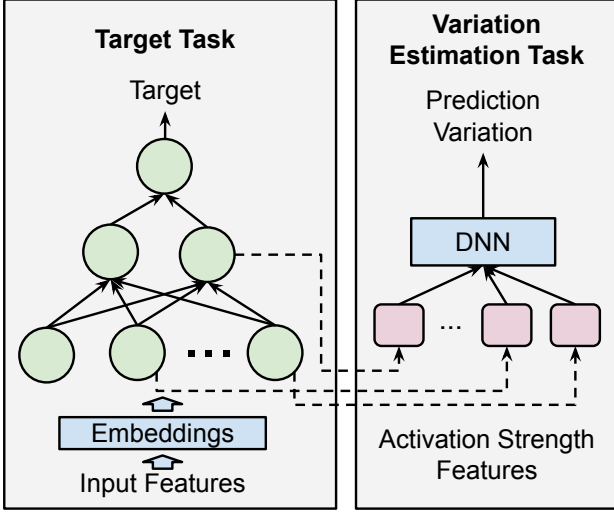


Figure 1: Our framework for prediction variation estimation using activation strength.

the large costs of training ensembles instead of a single model at the training stage of the auxiliary task model.

**Uncertainty estimation using dropout** is more resource-efficient than using ensembles as it does not require training multiple copies of the model. There are abundant studies [14, 15, 28] on dropout uncertainty estimation and its applications. For example, [14] proposed to use Monte Carlo (MC) dropout to estimate model uncertainty and established a connection to Bayesian inference. Further, they extended dropout to work with convolutions [13] based on the Bayesian connection. Concrete dropout [15] was introduced to automatically tune the dropout probability in large neural networks, avoiding costly searching for the optimal dropout hyperparameters. [37] evaluated MC-dropout and Concrete dropout for uncertainty estimation on semantic segmentation with proposed metrics. [36] studied MC-DropConnect and MC-Dropout as Bayesian methods in classification for segmentation settings with new uncertainty evaluation metrics. Further, [28] presented Bayesian SegNet with MC-Dropout to generate pixel-wise uncertainty estimation and image semantic segmentation tasks. Unlike the focus of prior work, our focus is on designing a proxy method that avoids the inference complexity of producing a dropout prediction variation score.

### 3 DROPOUT VARIATION ESTIMATION

Figure 1 shows the prediction variation estimation framework. As shown, it consists of two components: the target task and the variation estimation task. In this section, we introduce the setup of the two components.

**Target Task** — The target task represents the original prediction problem, such as the rating prediction on MovieLens [19]. It takes in the input features and predicts the target objectives. For example, on MovieLens, the target task takes in user and movie features, and predicts movie rating.

**Variation Estimation Task** — The variation estimation task takes in activation strengths from the target task model as its input features. Those features are concatenated into an input vector that feeds into a DNN to estimate the prediction variation for each input example. Dropout prediction variation (DPV) labels are collected by running multiple inferences on a target task with dropout enabled. They are then used to train the variation estimation task. After the training is complete, we no longer need to make multiple dropout inferences for prediction variation estimation. Instead, the trained variation prediction model estimates DPV from its inputs, the neuron activation strengths. The variation estimation task is a cheap auxiliary task alongside the target task that provides the dropout prediction variation estimation given an input example.

Next, we introduce two real-world configurations of the variation estimation task. We then give a formal definition of PV. We conclude this section by more detailed descriptions of how the neuron activation strengths are used.

#### 3.1 Variation Estimation Task Configurations

As shown in Figure 2, we consider two configurations for the dropout variation estimation task depending on whether the deployed target task is trained with dropout.

- **Configuration 1** describes a framework in which the deployed target task is trained with dropout enabled. At inference time, dropout is disabled. Neuron values post-activation (activation strengths) are collected, and then applies as inputs to the variation estimation task. PV labels are collected by running target task predictions multiple times with dropout enabled for a given example.
- **Configuration 2** describes a framework in which the deployed target task is trained without dropout. Many real-world production models avoid dropout in order to achieve better accuracy performance [8]. Again, neuron activation strengths are collected during the inference stage, and applied as input to the variation estimation task. A side target task is applied with dropout to gather PV labels by running multiple predictions for a given example during training of the auxiliary task. Inference in deployment uses only the target task without dropout and the trained variation estimation task.

Target tasks are run until convergence. For the most typical dropout setup, we apply dropout only to the fully-connected layers [14, 31]. In particular, we neither enable dropout on convolution layers on EMNIST, nor on embeddings [55].

#### 3.2 Prediction Variation

In this section, we now formally define dropout prediction variation. We run dropout inferences  $N$  times with neuron dropout rate  $r$ , for some predetermined rate  $r$ , either on the direct or side target task as in Figure 2. This process produces predictions  $\{\hat{y}_1(x), \dots, \hat{y}_N(x)\}$  for every training example  $x \in \{x\}$ .

For binary classification and regression, we define **prediction variation**  $PV(x)$  for an example  $x \in \{x\}$  and its predictions  $\{\hat{y}_1(x), \dots,$

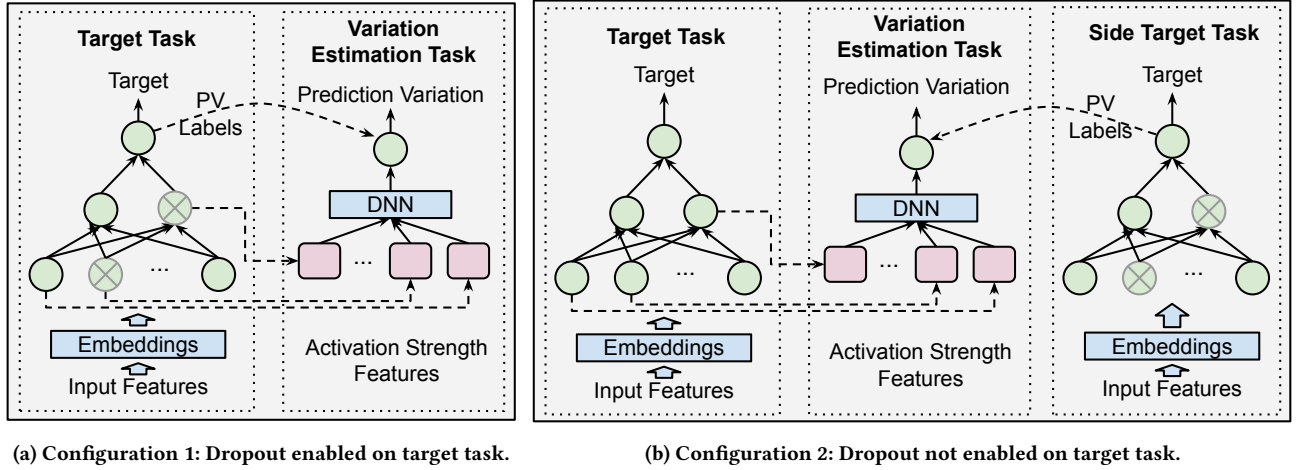


**Figure 2: Variation estimation task configuration for dropout prediction variations. PV labels represent the prediction variation labels, and the grey crossed neurons represent dropped neurons.**

$\hat{y}_N(x)$  to be the prediction standard deviation

$$PV(x) \triangleq \sqrt{\frac{\sum_{i=1}^N (\hat{y}_i(x) - \bar{y}(x))^2}{N-1}}, \quad (1)$$

where  $\bar{y}(x) = \frac{1}{N} \sum_{i=1}^N \hat{y}_i(x)$ .

For multi-class classification, the predictions for each input  $x$  over the  $N$  dropout inferences are a set of prediction label distributions  $\{\hat{p}_1(y|x), \dots, \hat{p}_N(y|x)\}$ . We use KL divergence based prediction variation defined as

$$PV(x) \triangleq \sum_{i=1}^N KL(\hat{p}_i(y|x) || \bar{p}(y|x)), \quad (2)$$

where  $\bar{p}(y|x) = \frac{1}{N} \sum_{i=1}^N \hat{p}_i(y|x)$  is the averaged prediction distribution over the  $N$  runs. We typically use  $N = 100$ .

### 3.3 Neuron Activations

The standard Rectified Linear Unit (ReLU) [38] activation is used in our models. ReLU fully de-activates neurons for which the input to the activation is negative. We can thus consider using activation outputs in two ways, either as binary or as the activation value. For the binary use, we only use an indicator of whether the neuron was activated or not as input to the variation estimation task. For the latter (full value use), the actual activation value of the neuron is used after normalization is applied.

A direct approach uses all neuron activations as inputs to the variation estimation task. However, this can lead to impractical input complexities, that may also underperform due to limited training data and overfitting. For example, the EMNIST target task model has layers of widths [3456, 1024, 120, 84], with a total neuron count of 4684. The variation estimation task with an initial hidden layer of width 100 will have 468K hidden link weights for just this first layer. The whole EMNIST dataset consists of only 280K examples, thus the variation estimation task will be highly overparameterized. Therefore, it may be better to use activations only from a subset of the hidden layers of the network. This reduces complexity as

well as potentially mitigates possible overfitting. Specifically, we have observed that if we used all the layers of the target task on the EMNIST dataset (including the convolutional layers), we obtained inferior predictions on the variation estimation task on validation data than when using all the fully-connected hidden layers (FCLs). We thus limit experiments in this paper to use activation inputs only from the FCLs to avoid overparameterization.

In addition, we want to further reduce the complexity and cost of variation estimation task by selecting a subset of FCL activation strengths. As different layers in a DNN reflect different representations of input data [48, 56], it might be possible to select the subset of neurons by layers. We demonstrate our findings in Section 5.2.

## 4 EXPERIMENT SETUP

### 4.1 Datasets

We consider three datasets to evaluate the proposed framework:

- **MovieLens** [19]: The MovieLens 1M dataset<sup>1</sup> is a benchmark dataset for evaluation of recommender systems. It features the task of using user and movie related features to predict movie ratings. This dataset contains 1M movie ratings of 4000 movies from 6000 users.
- **Criteo**: The Criteo Display Advertising challenge<sup>2</sup> features a binary classification task to predict Ads click-through rate. Labels are 1 for clicked examples, and 0, otherwise. This dataset has 40M examples.
- **EMNIST**: The EMNIST-Digits [7] dataset consists of a set of 280K handwritten images for a digit recognition task, which is an extension of the 70K MNIST [33] dataset.

**Training/Testing Data** — We set up the training and testing data for the target task and the variation estimation task by splitting the data into training  $D_{train}$  and testing  $D_{test}$  sets. EMNIST is split randomly into two equal sets, to ensure there are sufficient

<sup>1</sup><http://files.grouplens.org/datasets/movielens/ml-1m-README.txt>

<sup>2</sup><https://www.kaggle.com/c/criteo-display-ad-challenge>

(140K) test examples. MovieLens is split to 60% training and 40% test examples. For Criteo, we use the standard splitting [39], with 37M training examples and 4.4M validation and test examples. The test sets are further split randomly into two equal parts  $D'_{train}$  and  $D'_{test}$  for training and testing the variation estimation task.

## 4.2 Target Tasks Setup

We consider four target tasks on the three datasets all using multi-layer perceptron (MLP) architecture. For MovieLens and Criteo, the target task model contains a trained embedding layer connected to input features. For EMNIST, embeddings are not necessary.

**MovieLens Regression (MovieLens-R)** — The target task takes in user features (i.e., identification, gender, age, and occupation) and movie features (i.e., identification, title and genres), and predicts movie ratings as a regression task. The movie ratings are integers from 1 to 5. We use squared error as the loss function, and minimize the Mean Squared Error (MSE).

Each model is constructed with 3 fully-connected layers (FCL) of widths [250, 100, 50]. Each model trains for 20 epochs to converge. We use user ID and item ID embedding widths of 8 [22], user age embedding of width 3, user occupation embedding of width 5, and gender and genre features of one-hot encoding. We do not use the title textual feature for simplicity. Therefore, the total input embedding layer width is 43.

**MovieLens Classification (MovieLens-C)** — The same model as the one for the regression task is used here, except for the prediction objective. Instead of regression, the rating is treated as a multi-class classification to 5 integer value ratings (from 1 to 5). The model is thus trained to minimize Softmax cross-entropy loss.

**Criteo** — This target task uses 13 numerical and 26 categorical features that determine click-through-rate. High valency categorical features are encoded into embedding vectors, and low valency ones are hard encoded into one-hot vectors, taking a nonzero binary value for the category that is present. The overall input specifications follow those in [39]. The inputs feed into an MLP with layer sizes [250, 100, 50], which are trained with cross-entropy loss on  $\{0, 1\}$  labels (1 designating a click). The model output is mapped to a click probability using the Sigmoid function. The model is trained for one epoch with each example visited once.

**EMNIST** — This digit recognition task takes a  $28 \times 28$  pixels grayscale image representing a digit from 0 to 9, and predicts the digit in the image. We used the LeNet-5 [33] 10-category classification model. The model is composed of two convolutional layers with feature map sizes [3456, 1024], each followed by a max-pooling layer, and two FCLs of sizes [120, 84]. The model is trained over 50 epochs to converge.

All the above target tasks use Batch Normalization [25]. A batch size of 1024 is used for MovieLens and Criteo, and a batch of 128 is used on EMNIST [50]. We use Adam optimizer with initial learning rate 0.01 for Criteo, 0.1 for EMNIST, and 0.001 for MovieLens-C and MovieLens-R.

## 4.3 Variation Estimation Task Setup

As pointed out in Section 3.1, we use two configurations for the variation estimation task. The dataset slice  $D'_{train}$  is used to train the

variation estimation task and we use a 2-layer MLP with layer widths of [100, 50]. Inputs to the task are either all activation strengths of the fully-connected hidden layers of the target task, or activation strengths from subsets of the layers. Inputs can consist of activation values, and/or their binary indicators. We collect the dropout prediction variation labels by running dropout inference on the target task model or the side target task model 100 times. All the models are trained for 50 epochs. We use the Adam optimizer with initial learning rate 0.001, decaying by 0.1 at the 30-th and 40-th epochs. We repeat this process 20 times and report the average performance. Dataset slice  $D'_{test}$  is used to test the variation estimation performance. We show the target task accuracy performance for one dropout setting in Section 5 and under different dropout settings in Appendix B.

**Task Objectives** — The prediction variation estimation task is either a regression or a classification task.

- **Regression** — The model directly estimates the prediction variation using MSE as the loss function. By directly optimizing MSE, the output could have a substantial range. To mitigate this, we either clip or transform the outputs. With clipping, outputs are capped within the minimum and maximum measured prediction variation values. For EMNIST (as discussed in Section 5.1), we transform raw prediction and labels to log scale.
- **Classification** — For classification, prediction variation is uniformly divided by frequency into multiple buckets, and we predict the variation bucket. We use 5 buckets and cross-entropy loss. Bucket 0 is the most certain class and 4 the most uncertain one.

## 5 EXPERIMENTS

We report empirical results below. The results demonstrate that dropout prediction variation can be estimated with a DNN model that uses activation strengths as input. The results hold when we use all neurons of FCLs or a subset neurons of the FCLs as input features to the variation estimation task.

### 5.1 Variation Estimation

We first demonstrate the dropout prediction variation scores for the different datasets, and then show the performance of variation estimation task models. We study both configurations with dropout rates  $r = \{0.1, 0.2, 0.3, 0.4, 0.5\}$ .

**Dropout Prediction Variation** — Figure 3 shows histograms of dropout prediction variations for the four different tasks with dropout rate  $r = 0.1$ . Histograms are generated with 500 buckets for the measured dropout scores. The distributions of dropout prediction variations appear quite different for the different datasets. In particular, EMNIST exhibits a rather long-tailed distribution, with most examples having relatively low prediction variations, but with a substantial effect of outliers which have very large prediction variations. The target task is relatively easier to predict for most examples, and the variations in predictions are thus relatively low for those. However, there is a sufficient quantity of examples for which variations can be very large. We present more details in Appendix C.

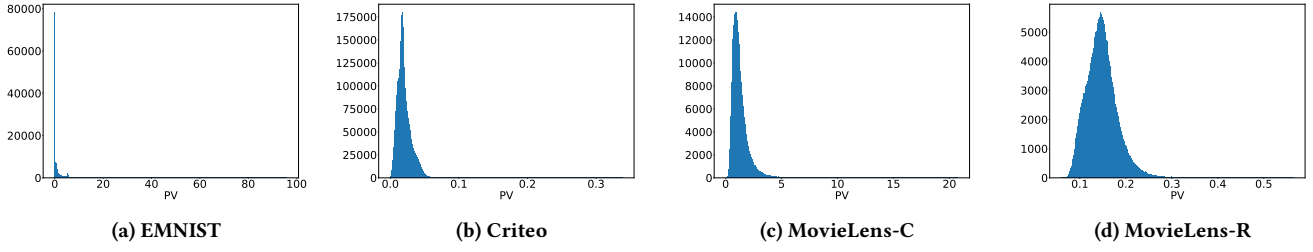


Figure 3: Prediction variation value distribution of different datasets when dropout rate is 0.1.

Target Tasks	Configuration 1					Configuration 2				
	0.1	0.2	0.3	0.4	0.5	0.1	0.2	0.3	0.4	0.5
EMNIST	0.513	0.574	0.554	0.542	0.456	0.450	0.494	0.445	0.441	0.307
Criteo	0.935	0.944	0.946	0.944	0.942	0.839	0.853	0.859	0.862	0.850
MovieLens-C	0.879	0.900	0.912	0.922	0.925	0.477	0.545	0.595	0.640	0.667
MovieLens-R	0.853	0.900	0.931	0.945	0.949	0.575	0.630	0.722	0.753	0.771

Table 1: Regression  $R^2$  of dropout prediction variation estimation for different configurations and dropout rates.

Target Tasks	Configuration 1					Configuration 2				
	0.1	0.2	0.3	0.4	0.5	0.1	0.2	0.3	0.4	0.5
EMNIST	0.530	0.497	0.463	0.429	0.463	0.471	0.447	0.418	0.384	0.411
Criteo	0.808	0.793	0.769	0.731	0.689	0.714	0.703	0.686	0.656	0.619
MovieLens-C	0.639	0.660	0.674	0.688	0.690	0.442	0.450	0.458	0.467	0.473
MovieLens-R	0.604	0.646	0.670	0.683	0.695	0.494	0.503	0.511	0.518	0.521

Table 2: Classification accuracy of dropout prediction variation estimation with different configurations and dropout rates.

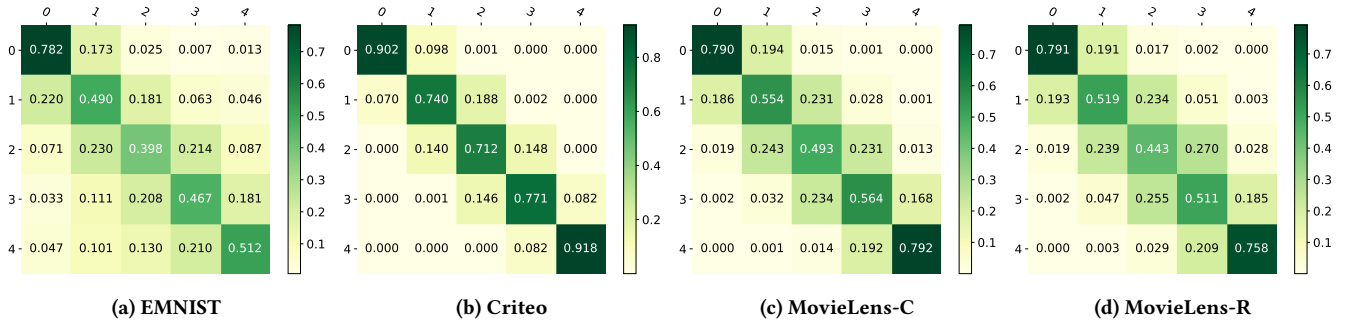


Figure 4: Confusion matrix of classification tasks for dropout prediction variation estimation with dropout rate 0.1. The rows and columns represent labels and predictions respectively.

**Dropout Variation Estimation** — Tables 1 shows  $R^2$  correlations between the predictions of the variation estimation task and the true dropout PV labels. Table 2 shows classification accuracy with 5 buckets for the two configurations in Figure 2. Figure 4 shows the confusion matrices for the classification task for Configuration 1 with dropout rate 0.1 for the different datasets. Results, qualitatively similar to Figure 4, are obtained with other dropout rates.

The results summarized in these tables and figures demonstrate that the variation estimation task is able to infer the actual PV

scores rather accurately in almost all cases. We observe  $R^2$  scores 0.5 or higher in most cases with regression and relatively high accuracy with classification, with the exception of EMNIST. As we observe in Figure 3, DPV for EMNIST is usually rather low. However, high DPV examples, while sparse, can have very large DPV. The extremely skewed DPV distribution has significant effects on the overall observed average metrics, degrading the quality of the prediction variation estimation task. Figure 6 in Appendix C demonstrates PV's for specific digit images in EMNIST, showing



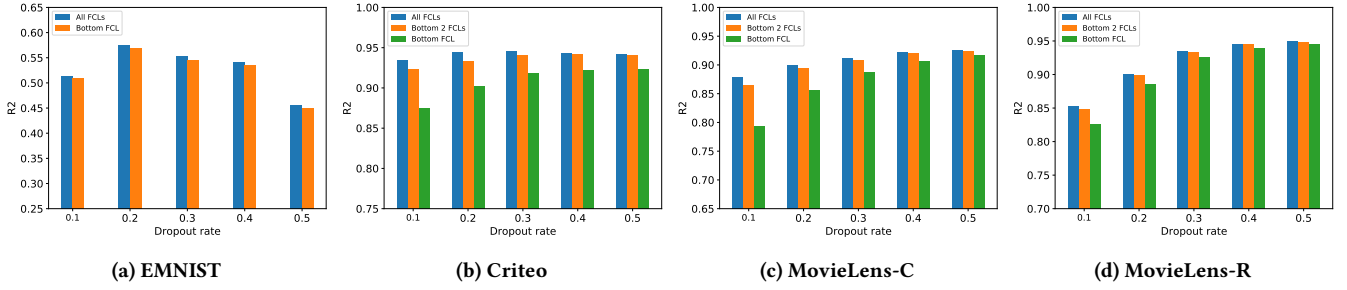


**Figure 5: Dropout prediction variation estimation performance using activations from different subsets of FCLs. The "All FCLs" bar is for inputs that include activations for all FCLs of the target model. For the "Bottom 2 FCLs" bar, inputs are from the two hidden layers closest to the input of the target task. For the "Bottom FCL" bar, inputs are taken only from the fully-connected input layer closest to the input of the target task.**

Target Tasks	All FCLs	Bottom 2 FCLs	Bottom FCL
EMNIST	45,850	-	29,050 (-36.6%)
Criteo	85,050	75,050 (-11.8%)	55,050 (-35.3%)
MovieLens-C	85,050	75,050 (-11.8%)	55,050 (-35.3%)
MovieLens-R	85,050	75,050 (-11.8%)	55,050 (-35.3%)

**Table 3: Parameter totals for variation estimation model with inputs from different combinations of FCLs.**

that the choice of the dropout rate and the actual digit can significantly affect the actual dropout PV. In Figure 4 we observe that the variation estimation model is able to predict the top and bottom PV buckets even more accurately than other buckets with accuracy close to 0.8 for MovieLens and even close to 0.9 for Criteo. This implies that if one wants to classify only extreme cases (i.e., the model predicts rather consistently on an example or in the opposite case, the model is very inconsistent for some example), using the low-complexity variation estimation task is almost as reliable as using the expensive multiple dropout method. Given the nature of the EMNIST dataset, the prediction accuracy of the variation estimation task for the most certain bucket is rather high (around 0.8). Because the most uncertain bucket has examples with very skewed DPV similar to overall DPV distribution, the accuracy is therefore limited for that bucket.

Dropout prediction variation of different dropout rates may be different. In fact, the correlations between the DPV's for different dropout rates may vary by dropout rates and datasets (see, e.g., Appendix D). Dropout rate should thus be tuned for the specific application. Our focus, in this paper, is on a cost-efficient method to provide DPV scores, and not on such tuning. Our empirical results suggest that DPV scores can be easily estimated with a simple forward propagation with inputs that are available from the target task, with no need for the high complexity of multiple inferences with multiple dropout paths for each example.

## 5.2 Layer Selection

The empirical results shown in Section 5.1 use activation strengths from all FCLs of the target task as inputs to the variation estimation model. Here we show that it is sufficient to use only a subset of

the layers, to further reduce the cost of estimating the DPV scores. Results are shown for Configuration 1, and we observe similar behaviors on Configuration 2.

Figure 5 shows  $R^2$  correlations between the DPV label and its estimate from the variation estimation model for the four target tasks, with dropout rate 0.1. Results are shown for three sets of inputs: a) activations in all fully-connected hidden layers, b) activations from the bottom two fully-connected hidden layer (where the bottom layer is the one closest to the inputs), and c) activations only from the bottom hidden layer. Using the bottom two layers exhibits almost no degradation from using all layers for all datasets. Using a single layer also achieves rather favorable results, with slight degradation relative to all layers. Similar results are obtained for other dropout rates.

Table 3 shows the reduction in the number of parameters by using only the bottom two or bottom layer relative to using all layers. For example, for EMNIST, using all layers, we use  $2 * 204 * 100 + 100 * 50 + 50 * 1 = 45850$  hidden parameters for the variation estimation task, which can take  $2 * 204$  inputs (204 neurons of both binary and value features), and feeds into a neural network model of sizes [100, 50, 1]. Using only the activations of the bottom fully-connected hidden layer, the complexity of the variation estimation model can be reduced by over 35%.

Further complexity reductions are possible by using inputs from layers with fewer neurons (closer to the output of the target task). Applying these inputs does show slight degradation in  $R^2$ , but not substantial. For example, we experimented with using neuron activation inputs from any single FCL on Criteo. The  $R^2$  correlations between the estimated DPV and the DPV labels were 0.882, 0.875, or 0.837 for the 250-neuron layer, 100-neuron layer, or 50-neuron layer, respectively.

Overall, our results demonstrate that by leveraging neuron activation strengths, our variation estimation task is able to reduce the need for multiple inferences for DPV estimation, as a cost-efficient auxiliary model. Moreover, our DPV estimates can be rather reliably obtained using even a single hidden neuron layer from the target task. A designer can tune the complexity to balance accuracy on the DPV estimation to fit the needs of their application.

## 6 DISCUSSION: DROPOUT VS. ENSEMBLE

Deep neural networks have complex loss landscapes with multiple local optima. Convergence to different optima is one cause of prediction variations that are described in Section 1. However, variations can be observed even if a training model is on track to converge to the same optimum but may have not reached it yet for some reason, e.g. early stopping, stuck at a local minima, oscillating around the optimum. Prediction variations can be due to data uncertainties, model misspecification, algorithm/optimizer suboptimality, training data sampling strategies, and other factors. A model can approach the same optimum or different optima from different directions, depending on initialization, order of training examples, schedule of its updates, random rounding errors, distributed training and parallelization, and even different software and hardware effects on the same algorithm. For example, some properties of a data center can affect order of operations which can result in one order in one data center and another in another.

A dropout prediction variation measurement for a given example is obtained from a distribution of predictions, each generated by a random selection of neurons to drop from the same model at the selected rate. Each selection of dropped out neurons effectively generates a slightly different model from the original model. Dropout in training attempts to ensure that the inference of a dropped out model is more robust and is still able to produce reliable predictions despite the dropout. Higher dropout rates introduce larger diversities. Table 5 in Appendix C demonstrates that by showing that with increased dropout rate both prediction variation mean and variance increase.

As the description of the dropout methodology suggests, dropout prediction variation score resembles an ensemble score (see also [13, 18, 46]). However, it is not quite clear which factors causing prediction variations are captured by ensemble scores and which are captured by dropout scores. With ensemble scores, the actual method used for diversifying the ensemble can, in fact, affect which effects are captured by the score and which are not. Dropout scores are clearly computed on “ensembles” whose components share some form of correlation that may not exist for independent ensembles. This correlation is due to the fact that the parameters of the original model were trained together and attributed credit among themselves, whereas this is not the case for ensembles. An ensemble whose components vary in initialization will exhibit different prediction variations from ensembles whose components were initialized identically, but had deviations due to other random factors (see, e.g., [45]). While it is clear that each of these scores measures effects of a different subset of all the causes of prediction variations, it remains an open problem to categorize which scores quantify which prediction variation cause.

## 7 CONCLUSION AND FUTURE WORK

We proposed and studied low-cost low-complexity prediction variation estimators that estimate prediction variations obtained by dropouts in a deep network. Dropout prediction variation measurements can be obtained by multiple inferences of a model on a single example, where each inference selects a different set of neurons to be dropped out. Our proposed estimator trains on such dropout prediction variation measurements and requires only a

single forward propagation at inference time. We demonstrated on three benchmark datasets that this estimator gives reliable estimates of the dropout prediction variation score without the need of multiple inferences. Empirical results showed a high correlation of the estimated scores to DPVs in regression mode, and high accuracy in classification mode, in which DPVs were clustered into buckets of different variation levels. These results were shown to be attainable even if only neurons from subsets of the network layers of the target task were used as inputs for the variation estimation task, and even when neuron activations from only a single layer of the target task were used. Our result is a proof of concept that a practical low-cost and low-complexity methodology can be used to output prediction variations (or uncertainty of predictions) for deep networks.

Future work could focus on the composition of the prediction variation sources, on how such compositions are reflected in different prediction variation scores, and on how estimation of such scores can be simplified. Understanding the differences between different scores can give rise to the ability to isolate each of the sources of prediction variation, perhaps to a point that will enable mitigation of such variations if necessary. It can also lead to identifying the sources in different applications (sources that may be different or may have different level of influence on the overall variations in different applications). It can also lead to better understanding of which types of estimators, like the one we proposed in this paper, are effective for which sources of prediction variation. Specifically, it would be beneficial to develop understanding of the differences between ensemble-based variation measurements and dropout variation measurements, as well as the differences within different techniques that are used for ensembles, and within different dropout strategies. Finally, generalizing our approach to problems, such as reinforcement and curriculum learning, is another interesting direction.

## REFERENCES

- [1] Omer Achrack, Raizy Kellerman, and Ouriel Barzilay. 2020. Multi-Loss Sub-Ensembles for Accurate Classification with Uncertainty Estimation. *arXiv preprint arXiv:2010.01917* (2020).
- [2] Zeyuan Allen-Zhu and Yuanzhi Li. 2021. Towards Understanding Ensemble, Knowledge Distillation and Self-Distillation in Deep Learning. *arXiv preprint arXiv:2012.09816* (2021).
- [3] Rohan Anil, Gabriel Pereyra, Alexandre Passos, Robert Ormandi, George E Dahl, and Geoffrey E Hinton. 2018. Large scale distributed neural network training through online distillation. *arXiv preprint arXiv:1804.03235* (2018).
- [4] Miguel Atencia, Ruxandra Stoean, and Gonzalo Joya. 2020. Uncertainty Quantification through Dropout in Time Series Prediction by Echo State Networks. *Mathematics* 8, 8 (2020), 1374.
- [5] Charles Blundell, Julien Cornebise, Koray Kavukcuoglu, and Daan Wierstra. 2015. Weight uncertainty in neural networks. *arXiv preprint arXiv:1505.05424* (2015).
- [6] Zhe Chen, Yuyan Wang, Dong Lin, Derek Zhiyuan Cheng, Lichan Hong, Ed H Chi, and Claire Cui. 2021. Beyond Point Estimate: Inferring Ensemble Prediction Variation from Neuron Activation Strength in Recommender Systems. In *Proceedings of the 14th ACM International Conference on Web Search and Data Mining*. 76–84.
- [7] Gregory Cohen, Saeed Afshar, Jonathan Tapson, and Andre Van Schaik. 2017. EMNIST: Extending MNIST to handwritten letters. In *2017 International Joint Conference on Neural Networks (IJCNN)*. IEEE, 2921–2926.
- [8] Paul Covington, Jay Adams, and Emre Sargin. 2016. Deep neural networks for youtube recommendations. In *Proceedings of the 10th ACM conference on recommender systems*. 191–198.
- [9] Alexander D’Amour, Katherine Heller, Dan Moldovan, Ben Adlam, Babak Alipanahi, Alex Beutel, Christina Chen, Jonathan Deaton, Jacob Eisenstein, Matthew D Hoffman, et al. 2020. Underspecification presents challenges for credibility in modern machine learning. *arXiv preprint arXiv:2011.03395* (2020).



- [10] Zach Eaton-Rosen, Felix Bragman, Sotirios Bidas, Sébastien Ourselin, and M Jorge Cardoso. 2018. Towards safe deep learning: accurately quantifying biomarker uncertainty in neural network predictions. In *International Conference on Medical Image Computing and Computer-Assisted Intervention*. Springer, 691–699.
- [11] Di Feng, Lars Rosenbaum, and Klaus Dietmayer. 2018. Towards safe autonomous driving: Capture uncertainty in the deep neural network for lidar 3d vehicle detection. In *2018 21st International Conference on Intelligent Transportation Systems (ITSC)*. IEEE, 3266–3273.
- [12] Stanislav Fort, Huiyi Hu, and Balaji Lakshminarayanan. 2019. Deep ensembles: A loss landscape perspective. *arXiv preprint arXiv:1912.02757* (2019).
- [13] Yarin Gal and Zoubin Ghahramani. 2015. Bayesian convolutional neural networks with Bernoulli approximate variational inference. *arXiv preprint arXiv:1506.02158* (2015).
- [14] Yarin Gal and Zoubin Ghahramani. 2016. Dropout as a bayesian approximation: Representing model uncertainty in deep learning. In *international conference on machine learning*, 1050–1059.
- [15] Yarin Gal, Jiri Hron, and Alex Kendall. 2017. Concrete dropout. *arXiv preprint arXiv:1705.07832* (2017).
- [16] Yarin Gal, Riashat Islam, and Zoubin Ghahramani. 2017. Deep bayesian active learning with image data. In *International Conference on Machine Learning*. PMLR, 1183–1192.
- [17] Jakob Gawlikowski, Cedric Njitecheu Tassi, Mohsin Ali, Jongseok Lee, Matthias Hunt, Jianxiang Feng, Anna Kruspe, Rudolph Triebel, Peter Jung, Ribana Roscher, et al. 2021. A survey of uncertainty in deep neural networks. *arXiv preprint arXiv:2107.03342* (2021).
- [18] Kazuyuki Hara, Daisuke Saitoh, and Hayaru Shouno. 2016. Analysis of dropout learning regarded as ensemble learning. In *International Conference on Artificial Neural Networks*. Springer, 72–79.
- [19] F Maxwell Harper and Joseph A Konstan. 2015. The movielens datasets: History and context. *Acm transactions on interactive intelligent systems (tiis)* 5, 4 (2015), 1–19.
- [20] Marton Havasi, Rodolphe Jenatton, Stanislav Fort, Jeremiah Zhe Liu, Jasper Snoek, Balaji Lakshminarayanan, Andrew M Dai, and Dustin Tran. 2020. Training independent subnetworks for robust prediction. *arXiv preprint arXiv:2010.06610* (2020).
- [21] Kaiming He, Xiangyu Zhang, Shaoqing Ren, and Jian Sun. 2016. Deep residual learning for image recognition. In *Proceedings of the IEEE conference on computer vision and pattern recognition*. 770–778.
- [22] Xiangnan He, Lizi Liao, Hanwang Zhang, Liqiang Nie, Xia Hu, and Tat-Seng Chua. 2017. Neural collaborative filtering. In *Proceedings of the 26th international conference on world wide web*. International World Wide Web Conferences Steering Committee, 173–182.
- [23] Matthew D Hoffman, David M Blei, Chong Wang, and John Paisley. 2013. Stochastic variational inference. *Journal of Machine Learning Research* 14, 5 (2013).
- [24] Gao Huang, Zhuang Liu, Laurens Van Der Maaten, and Kilian Q Weinberger. 2017. Densely connected convolutional networks. In *Proceedings of the IEEE conference on computer vision and pattern recognition*. 4700–4708.
- [25] Sergey Ioffe and Christian Szegedy. 2015. Batch normalization: Accelerating deep network training by reducing internal covariate shift. In *International conference on machine learning*. PMLR, 448–456.
- [26] Heinrich Jiang, Been Kim, Melody Guan, and Maya Gupta. 2018. To trust or not to trust a classifier. In *Advances in neural information processing systems*. 5541–5552.
- [27] Gregory Kahn, Adam Villafior, Vitchyr Pong, Pieter Abbeel, and Sergey Levine. 2017. Uncertainty-aware reinforcement learning for collision avoidance. *arXiv preprint arXiv:1702.01182* (2017).
- [28] Alex Kendall, Vijay Badrinarayanan, and Roberto Cipolla. 2015. Bayesian segnet: Model uncertainty in deep convolutional encoder-decoder architectures for scene understanding. *arXiv preprint arXiv:1511.02680* (2015).
- [29] Diederik P Kingma and Max Welling. 2013. Auto-encoding variational bayes. *arXiv preprint arXiv:1312.6114* (2013).
- [30] Balaji Lakshminarayanan, Alexander Pritzel, and Charles Blundell. 2017. Simple and scalable predictive uncertainty estimation using deep ensembles. In *Advances in neural information processing systems*. 6402–6413.
- [31] Nikolay Laptev, Jason Yosinski, Li Erran Li, and Slawek Smyl. 2017. Time-series extreme event forecasting with neural networks at uber. In *International conference on machine learning*, Vol. 34. 1–5.
- [32] Max-Heinrich Laves, Sontje Ihler, Tobias Ortmaier, and Lüder A Kahrs. 2019. Quantifying the uncertainty of deep learning-based computer-aided diagnosis for patient safety. *Current Directions in Biomedical Engineering* 5, 1 (2019), 223–226.
- [33] Yann LeCun, Léon Bottou, Yoshua Bengio, and Patrick Haffner. 1998. Gradient-based learning applied to document recognition. *Proc. IEEE* 86, 11 (1998), 2278–2324.
- [34] Andrey Malinin, Bruno Mlodozienec, and Mark Gales. 2019. Ensemble distribution distillation. *arXiv preprint arXiv:1905.00076* (2019).
- [35] Zelda E Mariet, Rodolphe Jenatton, Florian Wenzel, and Dustin Tran. 2020. Distilling ensembles improves uncertainty estimates. In *Third Symposium on Advances in Approximate Bayesian Inference*.
- [36] Aryan Mobiny, Pengyu Yuan, Supratik K Moulik, Naveen Garg, Carol C Wu, and Hien Van Nguyen. 2021. Dropconnect is effective in modeling uncertainty of bayesian deep networks. *Scientific reports* 11, 1 (2021), 1–14.
- [37] Jishnu Mukhoti and Yarin Gal. 2018. Evaluating bayesian deep learning methods for semantic segmentation. *arXiv preprint arXiv:1811.12709* (2018).
- [38] Vinod Nair and Geoffrey E Hinton. 2010. Rectified linear units improve restricted boltzmann machines. In *ICML*.
- [39] Yaniv Ovadia, Emily Fertig, Jie Ren, Zachary Nado, David Sculley, Sebastian Nowozin, Joshua Dillon, Balaji Lakshminarayanan, and Jasper Snoek. 2019. Can you trust your model’s uncertainty? Evaluating predictive uncertainty under dataset shift. In *Advances in Neural Information Processing Systems*. 13991–14002.
- [40] John Paisley, David Blei, and Michael Jordan. 2012. Variational Bayesian inference with stochastic search. *arXiv preprint arXiv:1206.6430* (2012).
- [41] Theodore Papamarkou, Jacob Hinkle, M Todd Young, and David Womble. 2019. Challenges in Markov chain Monte Carlo for Bayesian neural networks. *arXiv preprint arXiv:1910.06539* (2019).
- [42] Peter Schulam and Suchi Saria. 2019. Can you trust this prediction? Auditing pointwise reliability after learning. *arXiv preprint arXiv:1901.00403* (2019).
- [43] Gil I Shamir and Lorenzo Coviello. 2020. Anti-Distillation: Improving Reproducibility of Deep Networks. *arXiv preprint arXiv:2010.09923* (2020).
- [44] Gil I Shamir, Dong Lin, and Lorenzo Coviello. 2020. Smooth activations and reproducibility in deep networks. *arXiv preprint arXiv:2010.09931* (2020).
- [45] Robert R Snapp and Gil I Shamir. 2021. Synthesizing Irreproducibility in Deep Networks. *arXiv preprint arXiv:2102.10696* (2021).
- [46] Nitish Srivastava, Geoffrey Hinton, Alex Krizhevsky, Ilya Sutskever, and Ruslan Salakhutdinov. 2014. Dropout: a simple way to prevent neural networks from overfitting. *The journal of machine learning research* 15, 1 (2014), 1929–1958.
- [47] Cecilia Summers and Michael J Dinneen. 2021. Nondeterminism and Instability in Neural Network Optimization. *arXiv preprint arXiv:2103.04514* (2021).
- [48] Naftali Tishby and Noga Zaslavsky. 2015. Deep learning and the information bottleneck principle. In *2015 IEEE Information Theory Workshop (ITW)*. IEEE, 1–5.
- [49] Matias Valdenegro-Toro. 2019. Deep sub-ensembles for fast uncertainty estimation in image classification. *arXiv preprint arXiv:1910.08168* (2019).
- [50] Li Wan, Matthew Zeiler, Sixin Zhang, Yann Le Cun, and Rob Fergus. 2013. Regularization of neural networks using dropconnect. In *International conference on machine learning*. PMLR, 1058–1066.
- [51] Mingjian Wen and Ellad B Tadmor. 2020. Uncertainty quantification in molecular simulations with dropout neural network potentials. *npj Computational Materials* 6, 1 (2020), 1–10.
- [52] Yeming Wen, Dustin Tran, and Jimmy Ba. 2020. BatchEnsemble: An Alternative Approach to Efficient Ensemble and Lifelong Learning. *Eighth International Conference on Learning Representations (ICLR 2020)* (2020).
- [53] Andrew Gordon Wilson and Pavel Izmailov. 2020. Bayesian deep learning and a probabilistic perspective of generalization. *arXiv preprint arXiv:2002.08791* (2020).
- [54] Yi Yang, Zhigang Ma, Feiping Nie, Xiaojun Chang, and Alexander G Hauptmann. 2015. Multi-class active learning by uncertainty sampling with diversity maximization. *International Journal of Computer Vision* 113, 2 (2015), 113–127.
- [55] Tiansheng Yao, Xinyang Yi, Derek Zhiyuan Cheng, Felix Yu, Ting Chen, Aditya Menon, Lichan Hong, Ed H Chi, Steve Tjoa, Jieqi Kang, et al. 2021. Self-supervised Learning for Large-scale Item Recommendations. *CIKM* (2021).
- [56] Chiyuan Zhang, Samy Bengio, and Yoram Singer. 2019. Are all layers created equal? *arXiv preprint arXiv:1902.01996* (2019).

## A APPENDIX

## B TARGET TASK PERFORMANCE

Dropout usually has quality impact. It may reduces the effective number of parameters that a model can use to produce a prediction. Therefore, we summarize the inference quality on the target task of the dropped out model for different dropout rates for the different datasets in Table 4. Each entry in the table was evaluated with training 20 independent models, and each dropout inference was applied 100 times. Prediction quality is evaluated by accuracy for MovieLens-C and EMNIST, by AUC for Criteo, and by mean squared error (MSE) for MovieLens-R. For the first three datasets larger numbers imply better quality, and for the last set, smaller MSE implies better quality. As expected, quality degrades with larger dropout rates but it stays about the same without dropout at inference (but with dropout during training). Inference without

Target Tasks	Ensemble	Inference with Dropout					Inference without Dropout				
		0.1	0.2	0.3	0.4	0.5	0.1	0.2	0.3	0.4	0.5
EMNIST accuracy	0.992	0.990	0.986	0.982	0.975	0.962	0.993	0.992	0.992	0.992	0.991
Criteo AUC	0.799	0.797	0.796	0.793	0.790	0.787	0.799	0.798	0.798	0.797	0.795
MovieLens-C accuracy	0.471	0.469	0.468	0.467	0.464	0.459	0.472	0.473	0.473	0.472	0.470
MovieLens-R MSE	0.777	0.799	0.799	0.802	0.811	0.824	0.775	0.774	0.776	0.777	0.780

**Table 4: Target task performance for different dropout rates with dropout enabled in training and with and without dropout enabled in inference.**

Target Tasks		Ensemble		0.1		0.2		0.3		0.4		0.5	
		mean	SD	mean	SD	mean	SD	mean	SD	mean	SD	mean	SD
Classification	EMNIST	1.897	8.932	1.693	5.555	3.456	7.546	5.702	8.950	9.008	10.195	14.747	11.734
	MovieLens-C	4.488	3.096	1.265	0.758	1.694	0.925	2.113	1.111	2.599	1.346	3.235	1.653
Regression	Criteo	0.027	0.015	0.020	0.011	0.027	0.013	0.032	0.014	0.038	0.016	0.044	0.017
	MovieLens-R	0.179	0.058	0.146	0.034	0.148	0.042	0.161	0.055	0.177	0.068	0.199	0.079

**Table 5: The mean and standard deviation of dropout prediction variations for different dropout rates.**

dropout’s quality is also comparable to inference with an ensemble of size 100.

## C DROPOUT PREDICTION VARIATION

We study DPV measurements of the target tasks in more detail. Table 5 supplements Figure 3 showing the means and standard deviations of the DPV scores for the different target tasks over all training examples of  $D'_{train}$  of different dropout rates. Ensemble metrics of randomly-initialized and randomly-shuffled ensembles of size 100 components are shown for comparison. PV ranges are quite different for the different dropout rates and different tasks. The latter indicates that PVs are characterized by the statistics of the specific dataset. As one would expect, the distribution of PV widens with larger dropout rates, where both means and variances are increased. Variations shown in the top rows of Table 5 use the standard deviation PV defined in Equation 1. The bottom rows use the KL-divergence based PV defined in Equation 2. Orders of magnitude of the two are not comparable.

While most digits in EMNIST are usually easy to recognize, there are some special outliers that are easily misclassified. Those outliers lead to larger standard deviations in the DPV scores for EMNIST. Figure 6 shows prediction variation distribution of two different digits in EMNIST, which exhibit different behavior. Digit 0 is one that is usually easily recognized, while the digit 4 is easy to confuse with 9. Increasing dropout rate for 0 does not change the distribution of its PV, although stretches the deviation of outliers. The PV distribution for 4, on the other hand, exhibits very noticeable difference when dropout rate is increased.

## D DROPOUT PREDICTION VARIATION SENSITIVITY

It is interesting to study how different instantiations of the raw dropout prediction variation measurements correlate with each other. Suppose we run an experiment in which we train the target task model, then run inferences with random dropout on the same example for  $N$  times, and measure the prediction variation

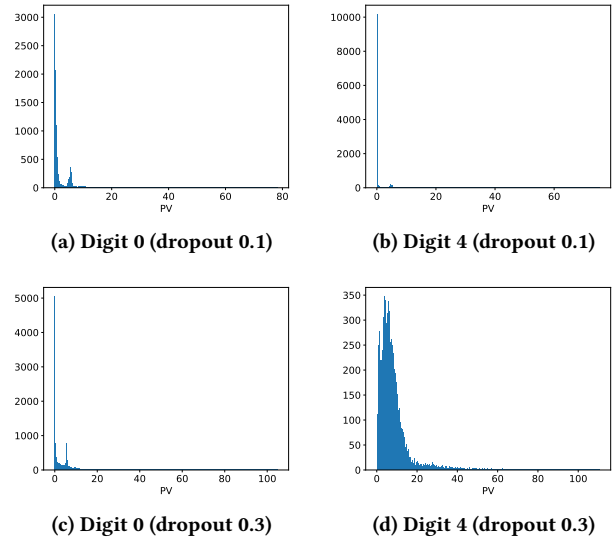


**Figure 6: Prediction variation distributions of digits 0 and 4 in EMNIST for dropout rate 0.1 and 0.3.**

distribution over all examples in a test set. Now, assume we repeat this experiment independently. In this section, we measure the correlations between multiple independent repetitions of such an experiment for a) the same dropout rate in each experiment, b) when dropout rates are different between two sets of experiments, and c) for different values of  $N$  for such experiments. These measurements give some indication of the sensitivity of the dropout score to a) random variations, b) dropout rate, and c) the amount of data used for the experiment (or data uncertainty of the prediction variation measurement itself).

Figure 7 reports  $R^2$  correlations between DPVs obtained with different dropout rates averaged over 20 independent runs with

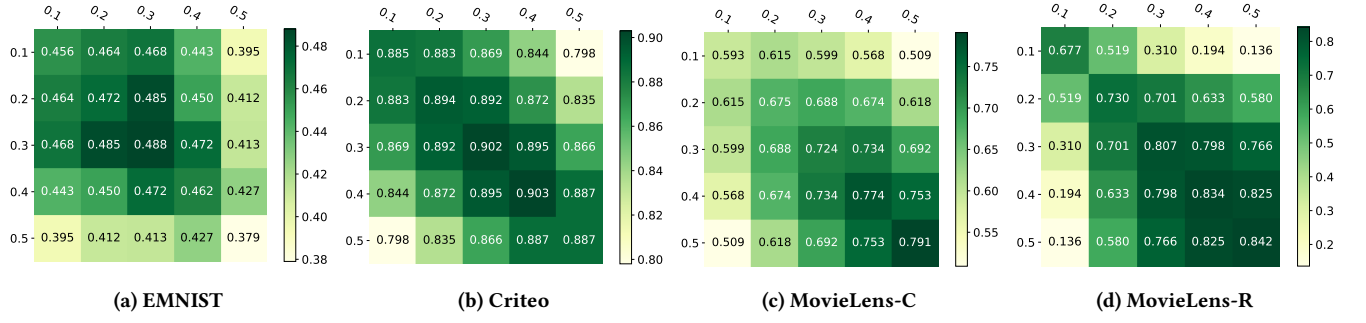


**Figure 7: Dropout prediction variation correlation of different dropout rates. The dropout prediction variation was collected by running dropout inference 100 times.**

different initialization, each with 100 independent dropout inferences, for the four different tasks. Correlations for the same dropout rate are measured with two retrains of a model. We observe, that dropout predictions for a pair of models with different dropout rates can be quite different. Larger rate differences usually reduce the correlations.

Finally, we consider the effect of the number of dropout inferences on the raw DPV measurements. Table 6 shows the correlation of the dropout prediction variation measurements between two independent experiments (as described above) on MovieLens-R where each experiments uses  $N \in \{10, 50, 100\}$  dropout inferences, for the different values of  $N$  and for different dropout rates. We observe

that, as one would expect, the prediction variation correlation tends to increase with increased number of inferences.

Number of Inferences	Dropout Rate				
	0.1	0.2	0.3	0.4	0.5
10	0.373	0.450	0.552	0.600	0.620
50	0.617	0.684	0.769	0.801	0.810
100	0.677	0.730	0.807	0.834	0.842

**Table 6: Dropout prediction variation correlation on MovieLens-R by running inference 10, 50, and 100 times for different dropout rates.**